Influence of the Anodization Process on Zamak 5 Corrosion Resistance

Ana Carolina Viero Bianchin[a], Sandra Raquel Kunst[b*] ⓘ, Luã Tainachi Mueller[a],

Jane Zoppas Ferreira[b], Fernando Dal Pont Morisso[a], Carlos Leonardo Pandolfo Carone[a],

Cláudia Trindade Oliveira[a]

[a]*Universidade Feevale, Instituto de Ciências Criativas e Tecnológicas (ICCT), RS 239, Bairro Vila Nova, CEP: 93352-000, Novo Hamburgo, RS, Brasil.*
[b]*Universidade Federal do Rio Grande do Sul, Programa de Pós-Graduação em Engenharia de Minas, Metalúrgica e de Materiais (PPGE3M), Laboratório de Corrosão, Proteção e Reciclagem de Materiais (LACOR), Av. Bento Gonçalves, Bairro Agronomia, CEP: 91501-970, Porto Alegre, RS, Brasil.*

Squeeze casting is the most industrially advantageous process for producing zamak 5 parts. However, this process generates porosity defects in parts, compromising their corrosion resistance. Therefore, this work aims to minimize defects and improve zamak 5 corrosive performance through the anodizing process. For this purpose, zamak 5 was anodized in 300 mol.m^{-3} oxalic acid and analyzed by ATR-FTIR, SEM, wettability and EIS techniques. The anodizing process promoted the formation of oxalate and oxide layers of Zn and Al, thereby reducing porosity defects. Although the anodized layer has fragile behavior, being porous and permeable, the immersion time of anodized zamak 5 in NaCl forms corrosion products in the alloy that exhibit better protection.

Keywords: *Zinc alloys, Zamak, Anodizing, Oxalic acid.*

1. Introduction

Zinc is a metal widely used either as metallic coating (galvanizing), as an alloying element (brass, zamak), in sacrificial anodes and as zinc oxide (chemical)[1]. In the Brazilian market, zinc consumption in 2017 was 2.51 x 10^8 Kg, and as zamak alloy, was 4.2 x 10^8 Kg, in which 48% of zamak is used in construction, 24% in the white line (valves; tools), 19% in the automotive sector and 9% in apparel and others as analyzed by Nexa's marketing team, Wood Mackenzie, 2018[2]. The name of the zamak series comes from the abbreviation of the names of the alloying elements that compose it: zinc, aluminum, magnesium and copper. These are hypoeutectoid zinc alloys, with aluminum contents around 4%, identified by numbers, such as zamak 5. For marketing, the squeeze casting is more advantageous because it allows to obtaining zamak parts with the same geometry, but with thinner walls than the casting in sand molds. This fact makes zamak 5 an important substitute for industrially used brass, because it enables mass savings of raw material without compromising the mechanical performance of parts. However, derived from the injection process, the surface porosity defect is one of the most that generates rejects in the industry. The porosity is due to the trapping of gases and vapors in the mold cavities[3,4]. Microporosity formation is also pressure dependent, although this is not the only factor influencing its presence[5,6]. Studies have shown that the corrosion resistance of the alloy is related to the presence of porosity defects[1,7].

To minimize these defects, increase corrosion resistance and provide a more attractive look, the industry uses surface finishing processes such as mechanical (polishing), acid copper electroplating, or the combination of both. However, these processes have not been satisfactory to minimize the porosity defect of zamak squeezed casting. In this sense, the anodizing process becomes a viable alternative, because it allows the anodized layer to form from the metal surface, thereby minimizing these defects.

Therefore, the objective of this work is to anodize squeezed casting zamak 5 to minimize porosity defects and improve corrosion resistance.

2. Experimental Procedures

2.1 Surface preparation

Prior to the anodizing process, the surfaces of the zamak 5 samples were prepared by sanding with silicon carbide (SiC) sandpaper in the following particle size sequence: 600, 800, 1200, 2400 and 4000 mesh. After the sanding process, the samples were polished with alumina paste on the buffing mandrel, Pantec brand, Polipan-U model, and washed with water for cleaning, in two different ways. In the first one, the samples were cleaned with alcohol only, rinsed with water and anodized. In the second one, the samples were submitted to the cathodic electrolytic degreasing, reproducing the process used industrially. The degreasing step was performed with application of 4.5 V for 45 seconds,

*e-mail: tessaro.sandra@gmail.com

washing in water followed by activation (in commercial product) for 20 seconds and again washed in water.

2.1.1 Anodization parameters

The anodizations were made using a 300 V – 0.5 A voltage source, coupled to a computer with data recording software. The process was started by applying a constant current density of 100 A.m^{-2} until the potential reached 100 V, going to constant potential of 100V[8] for 1800 seconds at room temperature.

In this work the samples were named according to the experimental conditions. ZP was named for the pure zamak sample, only submitted to the sanding and polishing process followed by water cleaning; Zatv means zamak subjected to electrolytic degreasing cleaning and activation and Zatv-30-G, zamak anodized for 1800 seconds and G corresponds to the graphite cathode. In this case, the experimental parameters of 1800 seconds and graphite cathode were used in order to approximate the anodizing to a process used industrially in the electroplating sector.

2.2 Surface characterization of anodized layer

Fourier transform infrared spectroscopy (ATR-FTIR) was initially performed to identify the functional groups formed on the surface of the anodized zamak. For this, the FTIR Spectrometer - Perkin Elmer (UART TWO) equipment was used in the region of 4 x 10^5 – 4 x 10^4 m^{-1}, with a resolution of 800 m^{-1} and a torque of 100 N.

Morphological analyzes were performed by scanning electron microscopy (SEM) on a JEOL-JSM-6510LV equipment with 20 keV acceleration voltage. In this case, the thickness, by cross section, and the surface of the anodized layer, in top view, were evaluated.

The film hydrophobicity was determined by the contact angle measurement from the sessile drop method in an equipment OCA 15EC, brand Labcontrol. In this analysis, a 4 x 10^{-4} m needle syringe with liquid deionized water was used, depositing 8.3 x 10^{-9} m^3 with a flow rate of 2.0 x 10^{-9} m^3/s.

The electrochemical behavior of anodized zamak 5 samples was performed on an AUTOLAB model PGSTAT 302 potentiostat. For this purpose, a three-electrode cell was used, which consisted of a saturated calomel reference electrode, a platinum counter electrode and a working electrode. The tests were performed in 600 mol.m^{-3} NaCl electrolyte simulating a corrosive medium. The sample area was 6.5 x 10^{-4} m^2 ± 2 x 10^{-5} m^2. Potentiodynamic polarization was made with a 1 x 10^{-3} V.s^{-1} scan

rate starting at - 0.2 V.s^{-1} up to + 1 V.s^{-1} with respect to the open circuit potential. Electrochemical Impedance Spectroscopy (EIS) measurements were performed in the frequency range of 1 x 10^5 Hz up to 3 x 10^{-3} Hz with 0.02 V sinusoidal signal. To evaluate the corrosive behavior of the samples, the impedance study was performed for 96 hours (345600 seconds), with analyzes every 24 hours (86400 seconds).

3. Results and Discussion

3.1 Anodization transients

Figure 1a and b shows the potential and current density transients of anodized zamak 5 samples in 300 mol.m^{-3} oxalic acid. For analysis purposes, the curve is illustrated up to 300 seconds.

At the beginning of anodization (1-a), a potential transient delay occurs which, according to Lilov et al.[9], was related to the induction period, with the formation of zinc crystals on the metal surface as a function of contact with the electrolyte. The induction period observed in this study was approximately 10 seconds using 300 mol.m^{-3} oxalic acid, in agreement with the results of Lilov et al.[9].

After the induction period, a continuous potential increase (up to 100 V) is observed up to approximately 120 seconds, generating a constant $(\partial V / \partial t)$ called the anodization rate[10]. In the same period (up to 120 seconds) the current density remains constant. After 120 seconds of anodization, the potential remains constant at 100 V and the current density decreases. This decrease in current density may tend to values near zero depending on the type of electrolyte, characteristic of barrier oxide formation. In the case of porous oxide formation, the current decreases, but the values do not tend to zero. According to Figure 1b, current density values decreased to low values, approximately 5 A.m^{-2}.

3.2 Fourier transform infrared spectroscopy (ATR-FTIR)

Figure 2 shows the ATR-FTIR spectrum in the region of 4000 to 400 cm^{-1} (4 x 10^5 – 4 x 10^4 m^{-1}) of the anodized zamak 5 sample.

The ATR-FTIR spectrum, Figure 2, of the anodized zamak 5 sample shows bands between 4000-400 cm^{-1} similar to those found by Lilov et al.[9], which used a typical spectrum of zinc oxalate dihydrate (ZnC$_2$O$_4$.2H$_2$O). Bands in the 4000-600 cm^{-1} region of the anodized sample (Figure 2) should be assigned to:
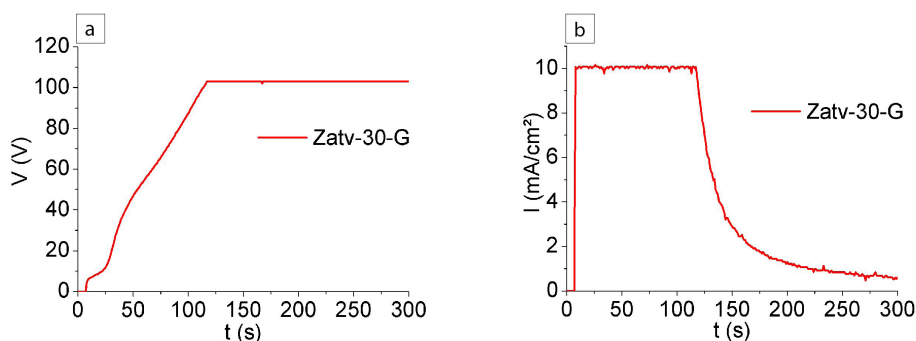

Figure 1. Potential (A) and current density (B) transients of anodized zamak 5 in oxalic acid.

3378.41 cm^{-1} (O-H stretching)), 1623,22 cm^{-1} (asymmetric C-O stretching), 1362,67 and 1316,79 cm^{-1} (symmetric C–O stretching + O–C–O bending), 820,08 cm^{-1} (symmetric C–C stretching coupled with O–C–O bending) e 744,70 cm^{-1} (O-H rocking).

In accordance with previous studies on hydrated metal oxalates[9], a band for the bending O-H mode of water was not observed due to the overlapping with the strong IR band of the asymmetric C-O stretching vibrations at 1620 cm^{-1}. In addition, bands were identified at 611.65 and 490.46 cm^{-1} for anodized zamak 5 (Zatv-30-G), Figure 2, which corresponds to the range between bands (600-500 cm^{-1}) providing information on the chemical bond between Zn and O[11,12]. Already the 451.50 cm^{-1} peak corresponds to ZnO [12] and the 490 cm^{-1} peak to the Zn-O and C-C[13] vibrational bands.

Therefore, it is observed that anodizing in zamak 5 forms zinc oxalate and zinc oxide in agreement with results observed by Lilov et al.[9]. On the other hand, as zamak 5 contains 4% Al in its chemical composition, which is presented as solute in zinc solid solution (β) and eutectic with two phases (β + α'), it is assumed that the observed bands may also be associated with aluminum oxalate or aluminum oxide.

3.3 Morphological characterization

Figure 3 shows the morphology of zamak 5 after the polishing process (ZP) (Figure 3a and Figure 3b) and after electrolytic degreasing (Zatv) (Figure 3c and Figure 3d).

The polishing process provides a smooth surface on the samples (Figure 3a), which was already expected. However,
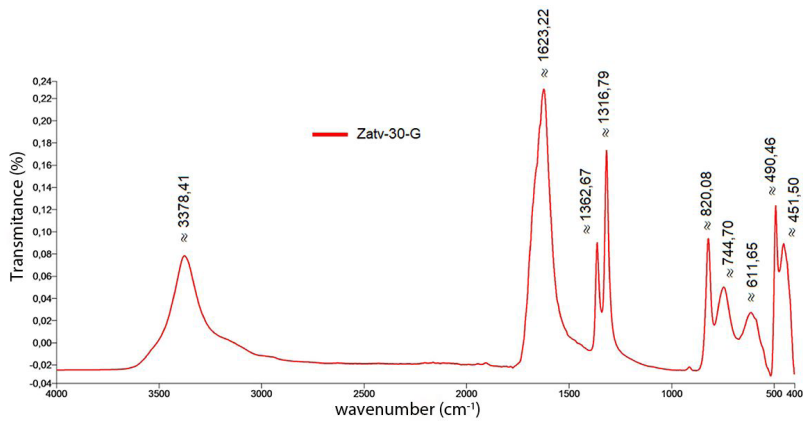

Figure 2. ATR-FTIR spectra of the anodized zamak 5 sample (Zatv-30-G) obtained in the region 4000 - 400 cm^{-1}.
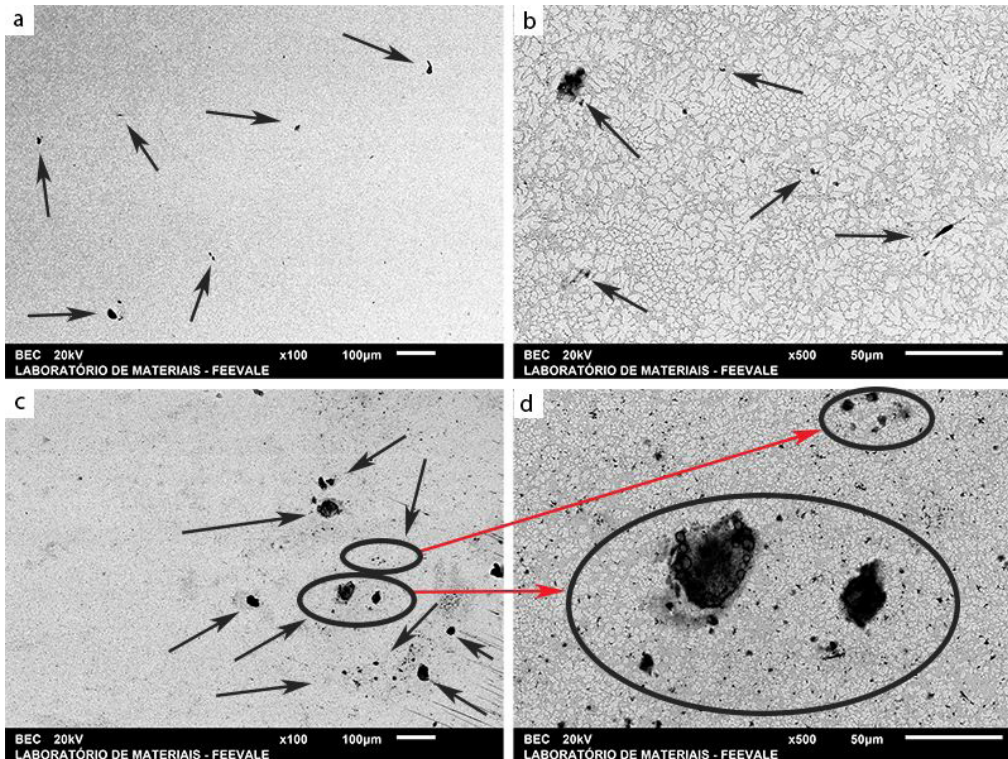

Figure 3. SEM micrographs of zamak 5 without electrolytic degreasing, ZP (a and b), and with electrolytic degreasing, Zatv (c and d).

squeeze casting induces the formation of porosities and worms on the surface of the zamak (indicated by the arrows, figure 3a-d) with variations in its dimensions. In greater magnification (Figure 3b) there is the characteristic microstructure of zamak with β-phase grains (rich in zinc) and the eutectic microstructure consisting of two phases β + α'[14-16].

Figure 4 shows top view micrographs of the Zatv-30-G, at different magnifications.

Figure 4 shows a surface containing crystallites, more clustered than those identified by Lilov et al.[9], and cracks.

According to Ferreira et al.[17], an initial zinc oxalate coverage occurs in samples immersed in oxalic acid, which is due to the electrolyte concentration. The authors verified that the highest coating coverage occurs at a concentration of 100 mol.m^{-3} oxalic acid and, increasing concentration to 1000 mol.m^{-3}, the coating dissolution occurs. The results obtained by the authors suggest that there is a competition between zinc dissolution in acid medium and zinc oxalate deposition, which is dependent on the concentration of oxalate and hydrogen ions on the zinc surface.

In addition, it must be considered that zamak contains 4% aluminum in its chemical composition, which may also have been anodized. The anodization of aluminum in 10% oxalic acid at 10 and 30 V potentials showed the formation of a porous oxide. The authors observed that anodizing done at potentials above 30 V showed the formation of oxide with high volume expansion, resulting in internal stresses in the leading the formation of cracks layer[18]. The same behavior was observed during the anodization of aluminum in 160 V, in H_3PO_4 with additions of oxalic acid. The volume expansion of the oxide was observed with an increase in the amount of oxalic acid to the electrolyte[19]. Therefore, the observed cracks may be due to the formation of zinc oxalate crystallites and due to volume expansion during the formation of aluminum oxide.

Figure 5 shows EDS chemical mapping analysis of Zp and Zatv-30-G samples obtained by SEM.

The EDS chemical mapping images, Figure 5, show aluminum on the surface of the anodized layer, which appears around zinc oxalate crystallites (Zatv-30-G).
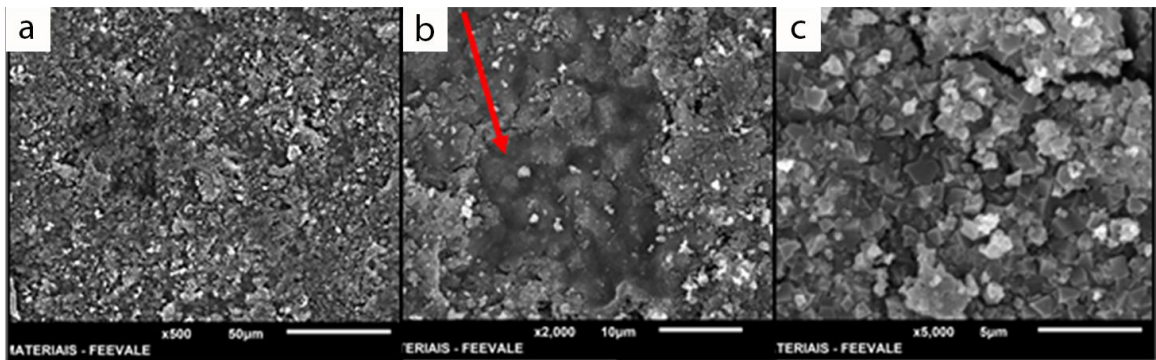

Figure 4. SEM micrographs of Zatv-30-G at magnifications of (A) 500x, (B) 2000x and (C) 5000x.
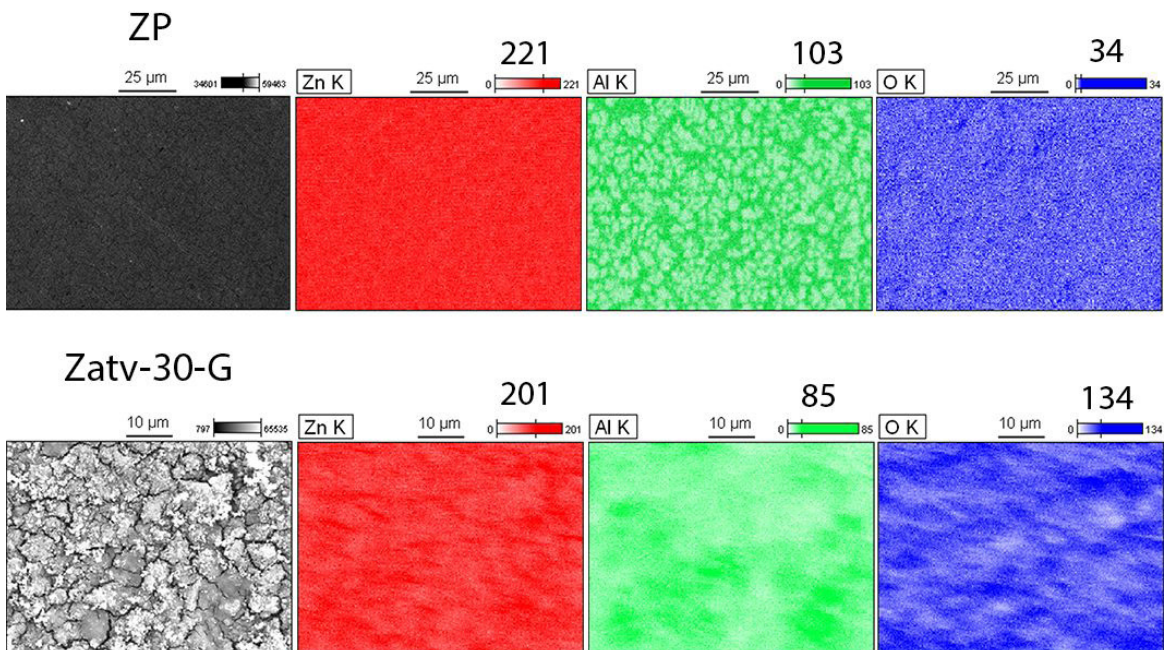

Figure 5. EDS chemical mapping of zamak 5 in top view (ZP and Zatv-30-G).

In anodizing aluminum in 300 mol.m^{-3} oxalic acid at 120 V, the authors showed that the phase formed is entirely amorphous Al_2O_3. The authors annealed this sample and the amorphous phase remained unchanged up to 700 ° C[20]. Another study on anodizing aluminum in electrolyte of 750 mol.m^{-3} of oxalic acid, with application of 45 V, for varied times of 60 to 150 minutes[21] showed the formation of porous oxide. The growth rate of the film was very fast, due to the high current density resulting from the high potential value. The electrochemical oxidation of aluminum at the base of the pores is controlled by diffusion as a consequence of the rapid growth of the oxide in high field conditions. Because of this rapid growth, it quickly depletes anionic species containing oxygen in the bottom of pores and a concentration gradient of anions along the narrow pore channels of aluminum oxide should be established[22]. In the case of this work, the oxalic acid electrolyte would be responsible for the anodization of aluminum, resulting in the depletion of the oxygen necessary for the formation of oxide (due to the high field), and for the formation of Zn^{2+} (due to the dissolution of Zn) which would combine with oxalate species to form zinc oxalate as a crystallite.

Further investigations have shown that the addition of approximately 5 wt% Al to molten Zn produces highly oxidation and corrosion resistant alloys due to the formation of a passive Al_2O_3 layer on its surface[23,24]. Therefore, one cannot disregard the hypothesis that aluminum has also been anodized as oxide.

Figure 6 shows the cross-sectional micrograph of the anodized zamak 5 sample for 30 min, Zatv-30-G.

It is observed that there is the formation of an oxide layer that accompanies the zamak surface. This confirms the growth of the anodized layer at the metallic interface/anodized layer and anodized layer / electrolyte, as observed by the growth from zinc grain, as shown in Figure 6. This layer growth is in accordance with the coverage of porosity defects originated during the zamak 5 squeeze casting process.

However, the coverage of the anodized layer was very irregular, showing failures and the thickness measured was approximately 2 x 10^{-6} m with standard deviation of 1 x 10^{-6} m. It is identified that only part of the oxide is adhered to the metal surface and part stands out. Studies have shown that aluminum anodizing in 300 mol.m^{-3} oxalic acid at 40 V in 300 seconds formed oxide 6 µm thickness[25]. Therefore, although the amount of aluminum in the zamak alloy is 4%, it can be inferred that part of the anodized layer is aluminum oxide. This behavior is in agreement with the images of Figure 4, where the anodized layer grows in the form of crystallites and presents morphology with cracks.

Figure 7 shows EDS chemical mapping in cross-sections of the zamak 5 anodized layers, Zatv-30-G.

It is observed, in the EDS chemical mappings of the cross sections, Figure 7, that there is the presence of zinc, aluminum and oxygen along the anodized layer. According to Goodwin and Rollez[24], zinc alloys, especially those containing aluminum and magnesium, form protective films of oxide and mixed salt, depending on the alloy composition. This statement justifies what was observed by means of ATR-FTIR (Figure 2), in which peaks of zinc oxalate and zinc oxide were observed that could possibly also be aluminum oxalate and aluminum oxide.
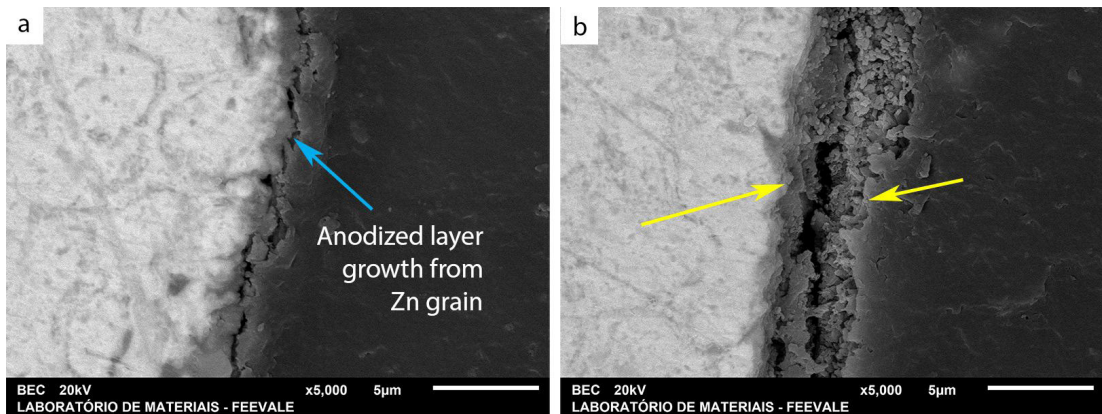

Figure 6. SEM cross-section micrograph of Zatv-30-G (a and b) in different regions.
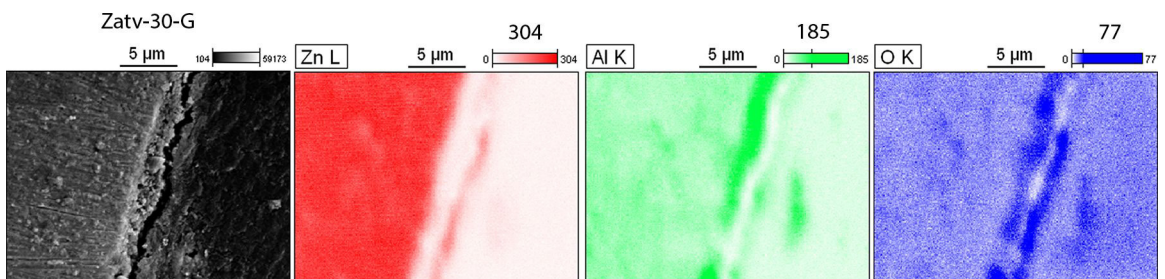

Figure 7. EDS chemical mapping in cross-section of Zamak 5 (Zatv-30-G) anodized layer.

It should also be considered that in the electrochemical series, Zn is anodic for Cu and Fe alloys and, depending on the specific conditions, is generally cathodic for Al and Mg[24]. This would explain the preferential formation of aluminum oxide over zinc, corroborating the SEM results that showed a region of crystallites, which possibly correspond to zinc oxalate, and a region that possibly corresponds to aluminum oxide (Figure 4).

3.4 Wettability analysis (contact angle)

Figure 8 shows contact angle images and values obtained by the sessile drop method of the zamak 5 ZP, Zatv e Zatv-30-G.

It is observed that the samples ZP and Zatv presented contact angle of approximately 110°, indicating that the surface has hydrophobic behavior.

According to Feliu and Barranco[26], in galfan (Zn-5%Al) coated steel samples, the formation of Al oxide on the outer surface of the coating obstructed the oxidation of Zn. Aluminum presents on both the outer surface and the inside of the coating appears to give rise to a thick Al_2O_3 film and consequently to make the surface hydrophobic. In the case of Zatv, the sample was dried after being electrolytically degreased, which justifies the behavior similar to that of the ZP sample, with the preferential formation of Al_2O_3 in air[27,28].

Already the anodized Zamak 5 sample presents a hydrophilic behavior, this is associated with the dissolution of zinc oxalate and the formation of Al_2O_3 in the anodized layer, which becomes fragile, porous and permeable, acting
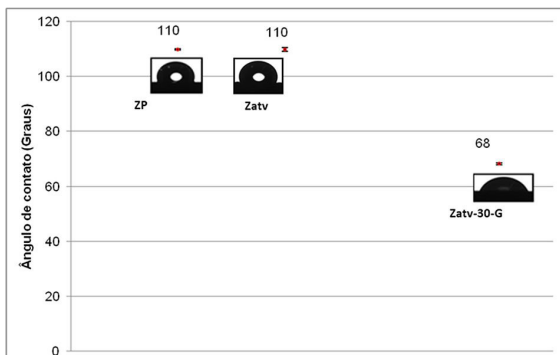
Figure 8. Contact angle images of the zamak 5 (ZP, Zatv e Zatv-30-G).
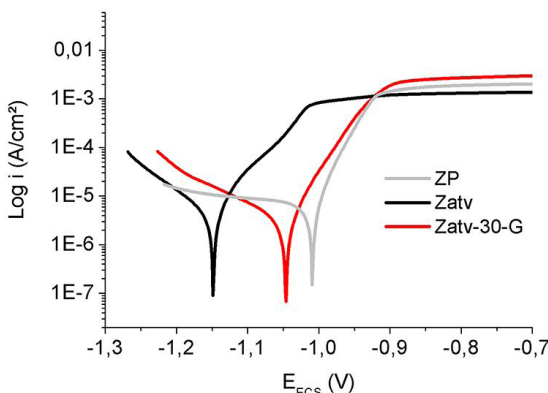
Figure 9. Potentiodynamic polarization curves of zamak 5 (ZP, Zatv e Zatv-30-G) in 0.6 M sodium chloride solution.

as a preferred pathway for wettability electrolyte. According to Gilani et al.[29] the contact angle is smaller for anodized zinc surfaces in NaOH and oxalic acid than for not anodized zinc, confirming that anodized surfaces are more hydrophilic on both electrolytes.

3.5 Electrochemical characterization.

Figure 9 shows the potentiodynamic polarization curves of the zamak 5 ZP, Zatv and Zatv-30-G samples in a 600 mol.m^{-3} sodium chloride solution.

It can be seen, Figure 9, that the ZP and Zatv samples showed more noble and less noble behavior, respectively, in relation to Zatv-30-G. ZP's most noble behavior with respect to Zatv may be due to the aluminum contained in zinc, forming an air-protective layer of Al_2O_3[27,28]. The ZP sample has a smaller cathodic Tafel slope compared to the other samples, indicating that the corrosion current is limited by the diffusion rate[30]. According to the author, the reaction rate is entirely controlled by the mass transport rate (but not potential), and by the cathodic Tafel slope value. Although both samples show similar hydrophobic behavior, in this analysis the Zatv sample was electrolytically degreased, washed with water, activated, cleaned in water and dipped directly into the electrochemical solution, without being dried, in order to verify the behavior of the samples under the same conditions of anodizing process. This behavior was observed by Fürh[7], who showed that zamak 5 presented typical pitting behavior with an open circuit potential of approximately -1 V, which is in agreement with the values obtained in Figure 9. The study by Mouanga et al.[31] shows that, in NaCl electrolytes, a passive layer is formed on the surface of the zinc electrode, composed of zinc oxide (ZnO), zinc hydroxide ($Zn(OH)_2$) and a hydroxide-zinc chloride complex ($Zn_5(OH)_8Cl_2.2H_2O$). The morphology of the oxide layer that grows under these conditions is not compact, being porous and fragile. Due to these characteristics, this formation is semi-passive. At the beginning of the anodic curve, there is an increase in the potential, from the corrosion potential, associated with a stability of the current density, reaching the current density limit. Notes that this behavior shows that the layer formed is not completely passive, but pseudo-passive[32]. In this case, if the layer were completely passive, there would be a decrease in the current density, which does not occur, agreeing with the hypothesis of formation of the zinc hydroxy-chloride, which is unstable, allowing the formation of a limit current.

For the anodized sample, there is a shift of the corrosion potential to less negative values compared to the Zatv sample. However, it is observed that the sample Zatv-30-G had similar corrosion potential to the ZP. This performance is associated with the fact that the anodized layer grows, breaks and continues the growth process, becoming more permeable, acting as the preferred path for the electrolyte and consequently decreasing its anti-corrosion performance. This result agrees with the SEM images (Figure 4) and wettability analyzes, in which hydrophilic behavior was verified (Figure 8).

Figure 10 shows the morphology of zamak 5 ZP (a and a1) and Zatv (b and b1) after the 600 mol.m^{-3} NaCl electrochemical
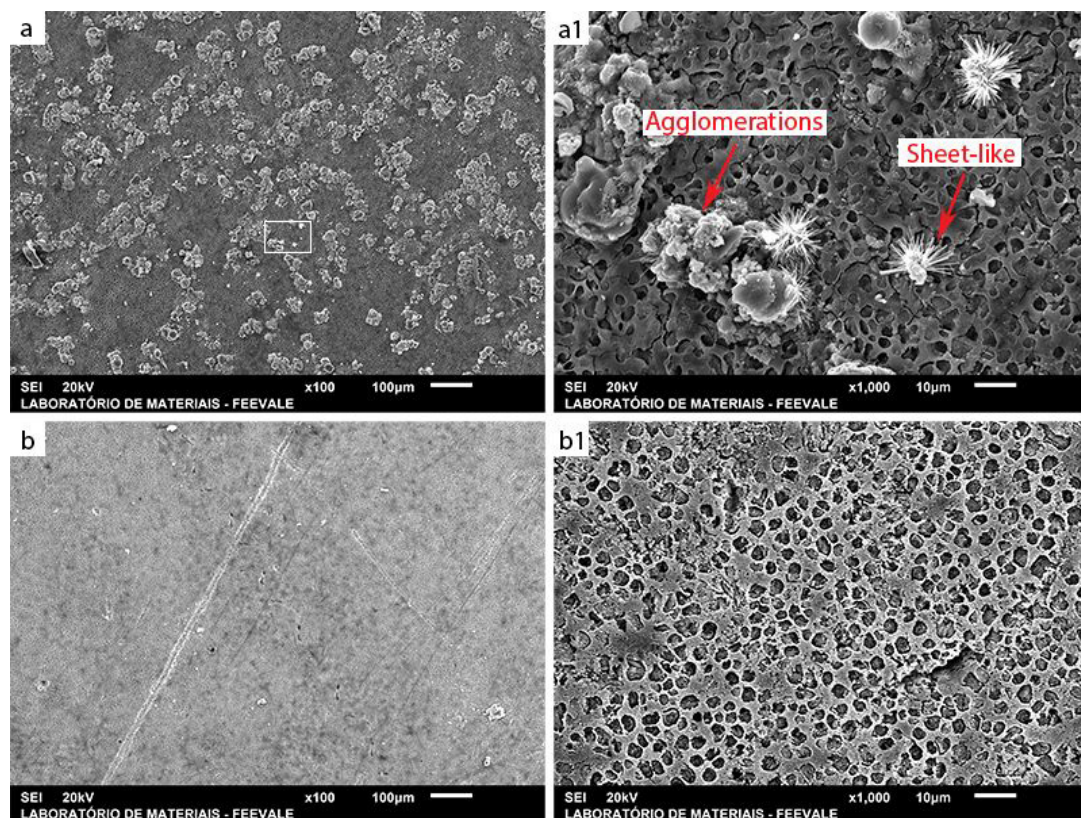
Figure 10. SEM micrograph of zamak 5 ZP (a and a1) and Zatv (b and b1) after polarization at magnifications of (a and b) 100x, (a1 and b1) 1000x in 0.6 M NaCl.

polarization test, where ZP (a1) is an enlargement of the labeled part in ZP (a).

Figure 10 (a1 and b1) shows irregular morphology containing pitting-like porosities originated during the polarization test. In the ZP sample, corrosion product is observed on its surface, which is not observed in Zatv. According to Cao et al.[27], samples of Zn-5Al showed, after 2 h (7200 seconds) of NaCl immersion, a small amount of sheet-like corrosion products with small agglomerations, similar to Figure 10 (a1). As in this work, the corrosion product observed by Cao et al.[27] did not cover the entire length of the sample, containing a eutectic lamellar structure ($\beta + \alpha$ ') and a proeutectic phase (β) of zinc. The author justifies that the corrosion product develops preferentially around the proeutectic zinc area which is the preferred area for corrosion product formation. Therefore, the corrosion products identified in the images (Figure 10, ZP(A-A1)) resemble those found by Cao et al.[27]. According to the authors, the aluminum content in the corrosion products in some regions is higher than others, indicating that the protective ability of the Al_2O_3 film on the surface of Zn-5Al alloy is relatively weaker, and the dissolution of Al involves the formation of corrosion products. The products composed mainly of zinc indicate that the β-Zn phase is the main phase to be corroded. Therefore, as the aluminum content of corrosion products in some regions is higher, both the α'-Al and β-Zn phases anticipate the corrosion at this stage. In this case, sheet-like corrosion products may be Cl$^-$ rich,

such as $Zn_5(OH)_8Cl_2 \cdot H_2O$ and cluster-like corrosion products are possible $Zn_6Al_2(OH)_{16}CO_3 \cdot 4H_2O$ or ZnO[27].

On the other hand, in the Zatv sample these corrosion products are not observed, which is in accordance with the removal of dirt and oxides on the surface, including the removal of air-formed Al_2O_3, caused by alkaline degreasing.

Figure 11 shows the SEM morphology of the anodized Zatv-30-G (b and b1) sample after the polarization measurement in 600 mol.m^{-3} NaCl solution.

Figure 11 shows that, in the anodized Zatv-30-G sample, the corrosion seems to be deeper and more punctual compared to ZP and Zatv (Figure 10), starting at the cracks of the anodized layers, as observed by SEM. According to Cao *et al.*[27], Zn-5Al forms breaks/cracks around the non-uniform corrosion product over the immersion time.

Figure 12 shows the Bode impedance spectra: Modulus (a) and Phase (b) of zamak 5 (ZP) in the immersion period of 24h, 48h, 72h and 96 h in a solution of 600 mol.m^{-3} sodium chloride.

The ZP sample, Figure 12b, presents, in 1h of immersion, three time constants, at high, medium and low frequency. The high frequency phenomenon can be associated with aluminum oxide formed instantly in air[28]. According to Liu et al.[33] and Cao et al.[27], the first high frequency time constant refers to the properties of the corrosion product layer, which in this case is due to air-formed Al_2O_3. The medium frequency phenomenon is associated with the permeability of the electrolyte in the probable corrosion product already formed, which means permeability in the
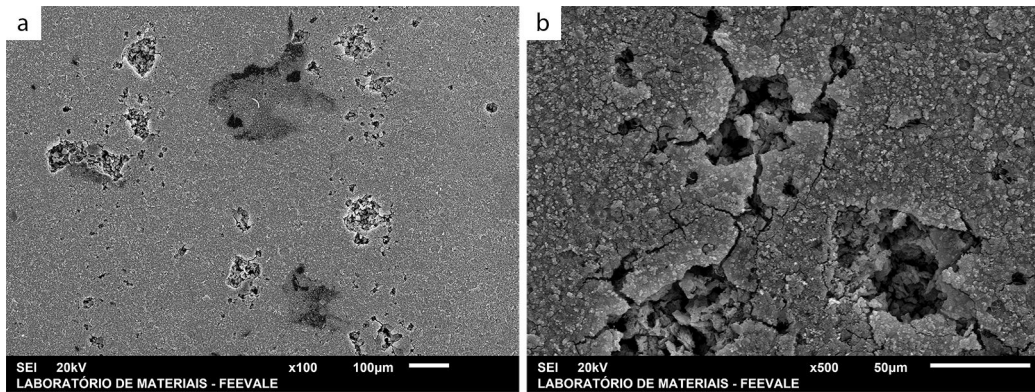
Figure 11. SEM micrograph of zamak 5 (Zatv-30-G) after polarization (b and b1) at 100x and 500x magnifications in 0.6 M NaCl.
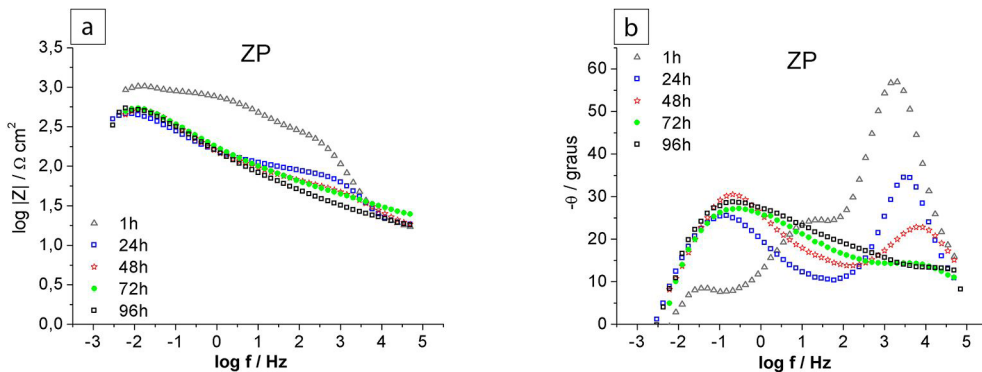

Figure 12. Electrochemical impedance spectra of Bode: Modulus (a) and Phase (b), measured on corrosion potential of zamak 5 (ZP) in 0.6 M NaCl.

aluminum oxide formed in the air, and the low frequency constant can characterize the corrosion process that occurs at the corrosion product interface with the alloy. In this case, the low frequency constant may be associated with the low thickness of the air-formed oxide.

According to Figure 12b, with increasing immersion time, the high frequency phenomenon decreases the phase angle up to 48h and disappears from 72h. The medium frequency phenomenon disappears after 24h of immersion and the low frequency phenomenon increases the phase angle from 24h of immersion and stabilizes by approximately 30°. According to Cao et al.[27] the high frequency constant corresponds to the properties of the corrosion product, which is related to the air-formed oxide, which has no protective properties when exposed to NaCl for prolonged immersion times. Already the medium frequency phenomenon corresponds to the increase of the permeability of the electrolyte, causing the corrosion product formation, which can be seen with the increase of the low frequency phenomenon. The time constant at low frequencies is characterized by the corrosive process at the corrosion product/alloy interface, so that impedance values decreased with anodizing time, reducing corrosion resistance according to the impedance modulus spectrum, Figure 12a.

Figure 13 shows the Bode impedance spectra: Modulus (a) and Phase (b) of zamak 5 (Zatv) in the immersion period of 24h, 48h, 72h and 96h in 600 mol.m^{-3} solution of sodium chloride.

Figure 13b shows that in 1h of immersion, the Zatv sample presents two well-defined time constants, at high

and low frequency. The high frequency phenomenon of Zatv, observed in 1h of NaCl immersion, resembles the high frequency phenomenon of ZP in 24h of immersion, which indicates that the Zatv sample doesn't have air-formed Al$_2$O$_3$, due to electrolytic degreasing, thus forming corrosion product at this time of immersion. On the other hand, the low frequency phenomena shows a higher angle in Zatv sample than in ZP. In addition, the Zatv impedance modulus showed little variation with the immersion time compared to the ZP (Figure 12a).

Figure 14 shows the Bode impedance spectra: Modulus (a) and Phase (b) of zamak 5 (Zatv-30-G), in the immersion period of 24h, 48h, 72h and 96h, in 600 mol.m^{-3} sodium chloride solution.

In 1h of immersion, it is observed that the Zatv-30-G sample, Figure 14b, presents two time constants, at medium and low frequency. However, the medium frequency phenomenon shows a 45° phase angle, known as Warburg impedance, which is reported as a controlled diffusion of the corrosive process occurring on the anodized surface[17]. This behavior is associated with an internal tension that occurs at the interface of the crystallites during the formation of the anodizing layer, causing its embrittlement and breaking, resulting in preferential paths for electrolyte's diffusivity. In addition, a phase angle of 45° is observed which, according to Cao et al.[27], is due to the change in corrosion kinetics from charge transfer control to diffusion control, called Warburg.
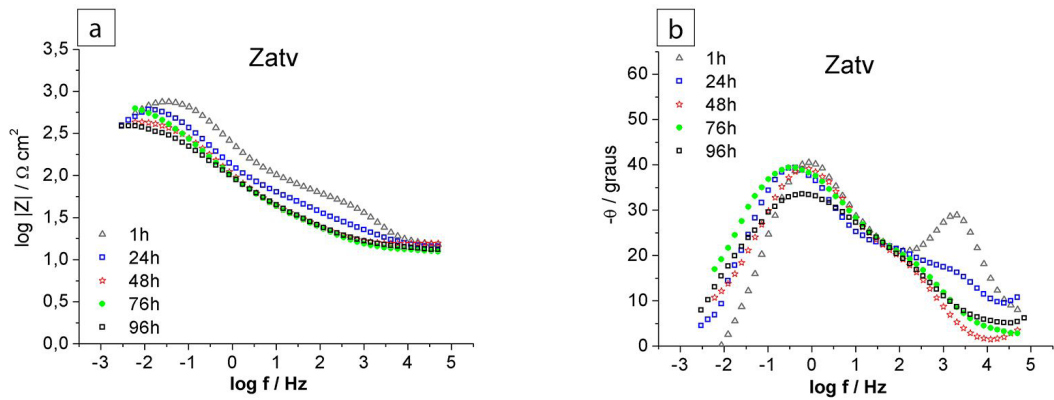
Figure 13. Electrochemical impedance spectra of Bode: Modulus (a) and Phase (b), measured on the corrosion potential of zamak 5 (Zatv) in 0.6 M NaCl.
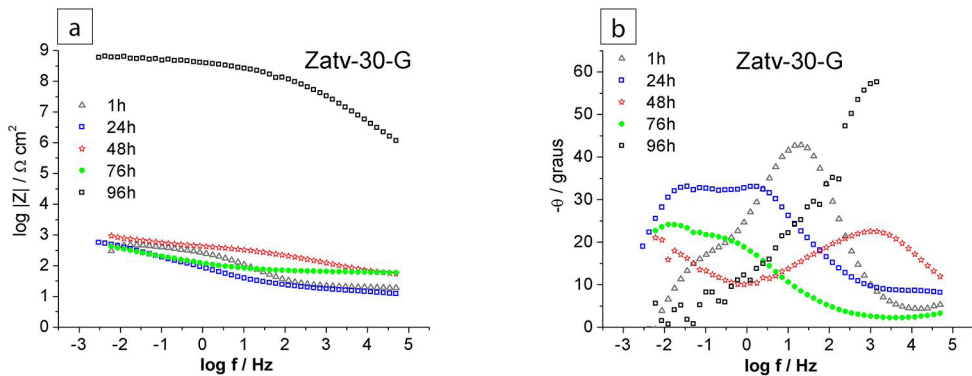

Figure 14. Electrochemical impedance spectra of Bode: Modulus (a) and Phase (b), measured on the corrosion potential of anodized zamak 5 (Zatv-30-G) in 0.6 M NaCl.

At 24 hours of immersion, the peak is no longer observed at medium frequency, which may be associated with the dissolution of the anodized layer. However, there is a low frequency phenomenon associated with the corrosive process. At 48h, there is a high frequency phenomenon with low phase angle, which may be associated with the corrosive process to form Al_2O_3, which temporarily protects. After that, Al_2O_3 dissolves itself again, which can be observed in 72h of immersion when the high frequency phenomenon disappears. This phenomenon is again observed in 96 hours of immersion, showing that corrosion products in Zatv-30-G exhibit better protection.

Figure 15 shows the morphology after 96 hours of immersion in 600 mol.m^{-3} of NaCl in the electrochemical impedance spectroscopy test for the ZP, Zatv and Zatv-30-G samples as well as the chemical mapping to the EDS of the Zatv -30-G sample after 96 hours of immersion in electrochemical impedance test.

It is observed in the images and micrographs of Figure 15a that the non-anodized sample ZP presents a generalized corrosion product. This result is in accordance with the impedance spectra (Figure 12) in which this sample showed a time constant at low frequencies, characterized by the occurrence of the corrosive process at the corrosion product/alloy interface.

Apparently, it is noted that there is more corrosion product in ZP, with agglomerates than in Zatv (Figure 15b), which agrees with the results of electrolytic degreasing in this sample, with the removal of corrosion products. This corroborates the impedance results (Figure 13) in which the low frequency phenomena present a greater angle in the Zatv sample than in the ZP, which is identified in the greater amount of corrosion product formed in Zatv (Figure 15b) in comparison to ZP (Figure 15a). Furthermore, Zatv impedance modulus showed little variation with the immersion time compared to ZP.

For the anodized sample (ZATV-30-G), there is a greater coverage of corrosion products (Figure 15c) compared to non-anodized samples. In the mapping of the chemical elements, Figure 15d, there is an increase in the amount of aluminum, zinc and oxygen, corroborating the greater formation of corrosion products of Al_2O_3, which temporarily protects. In this process, a preferential dissolution of the zinc corrosion product occurs and preferential formation of the aluminum corrosion product, since the anodized layer containing Al, which is supposed to be Al_2O_3, presents a more noble behavior compared to zinc oxalate, which is soluble in water. As a result, corrosion products cover the entire anodized layer including cracks, helping to resist corrosion. This behavior was already expected, since the impedance
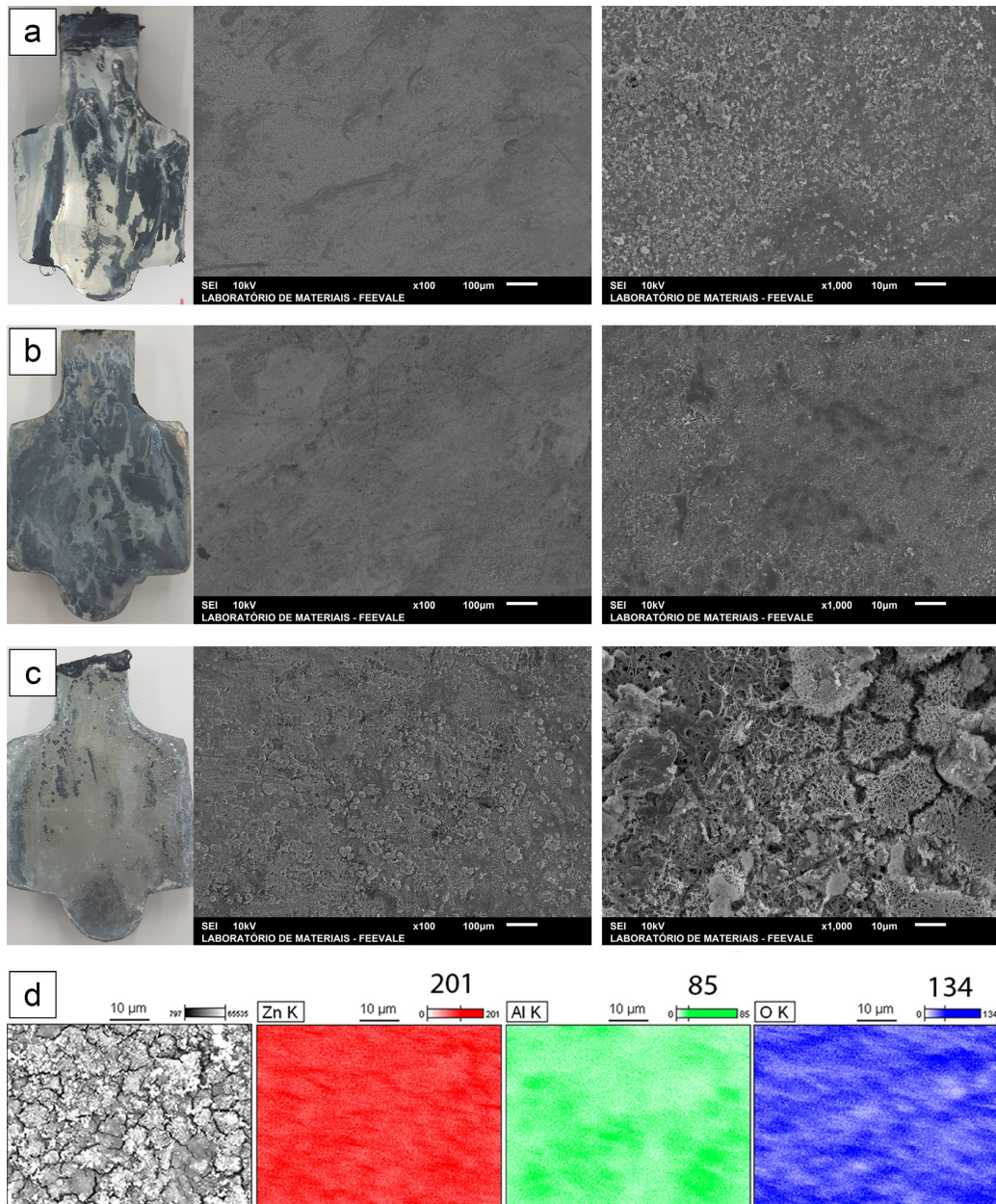
Figure 15. Sample morphology (a) ZP, (b) Zatv, (c) Zatv-30-G and (d) chemical mapping to the EDS of the Zatv-30-G sample after 96 hours of immersion in the electrochemical impedance test.

tests (Figure 14) showed a phenomenon in high frequency in 96h of immersion in the anodized samples, improving the resistance to corrosion. These results are in agreement with Cao et al.[27], who found in his study that the resistance of the corrosive product layer, at the end of the test, was higher. The authors proposed that the corrosion products in the Zn-5Al0.06Nd alloy exhibit better protection, that is, the longer the immersion time, the greater the corrosion resistance. In addition, they verified that there was a compaction of the layer due to the formation of corrosion products, and consequently obtained better resistance to corrosion. This is in accordance with the images in Figure 15c, in which it is observed that the corrosion was less intense to ZATV-30-G than ZP (Figure 15a) and Zatv (Figure 15b).

4. Conclusions

The anodizing process in 300 mol.m^{-3} oxalic acid formed a layer on the surface of zamak 5 that reduced porosity defects. The anodized layer is composed of Zn, Al and O as oxalate and oxide. The morphology of the anodized layer presents crystallites associated with oxalate de zinc and regions associated with aluminum oxide. The formation of the anodized layer occurs by a process of forming aluminum oxide of zinc dissolution, forming Zn^{2+} which combines with oxalate species of the electrolyte forming zinc oxalate. In addition, the anodized layer contains cracks, which was associated with the volume expansion of the aluminum oxide formed by anodizing, making the layer fragile, porous and

permeable, acting as a preferred pathway for wettability electrolyte. The sample Zatv-30-G had similar corrosion potential to the ZP. This performance is associated with the fact that the anodized layer grows, breaks and continues the growth process, becoming more permeable, acting as the preferred path for the electrolyte and consequently decreasing its anti-corrosion performance, agreeing with the results of contact angle. The SEM images after polarization in the anodized Zatv-30-G sample, shows that the corrosion seems to be deeper and more punctual compared to ZP and Zatv, starting at the cracks of the anodized layers.

The impedance tests showed that zamak (ZP) does not present protective properties with the exposure time in NaCl. The Al_2O_3 oxide formed in air is very thin, causing the formation of corrosion products, which are permeable with the time of immersion. However, the Zatv sample doesn't have air-formed Al_2O_3, due to electrolytic degreasing, thus forming corrosion product at 24h time of immersion in NaCl. For the anodized Zatv-30-G sample, corrosion products are formed in the sample cracks, which may be associated with the corrosive process to form Al_2O_3, which temporarily protects. With the time of immersion, this corrosion product dissolves and returns to form, showing better protection in 96 hours compared to non-anodized samples. In this process, a preferential dissolution of the zinc corrosion product occurs and preferential formation of the aluminum corrosion product, since the anodized layer containing Al_2O_3, presents a more noble behavior compared to zinc oxalate. As a result, corrosion products cover the entire anodized layer including cracks, helping to resist corrosion.

5. Acknowledgments

6. References

1. Marcolin P, Longhi M, Zini LP, Kunst SR, Zattera AJ, Fuhr LT, et al. Effects of the casting temperature in the Leakage of Zamak 5. Mater Sci Forum. 2017;899:458-62.

2. Wood Mackenzie. Nexa's marketing team analysis. Edinburgh: Wood Mackenzie; 2018.

3. Yoshino NY, organizador. Manual de fundição sob pressão. São Paulo: Grupo Votorantim Metais; 2010.

4. Malavazi J. Votorantim metais: manual de fundição sob pressão. São Paulo: Grupo Votorantim Metais; 2015.

5. Ghomashchi MR. High-pressure die casting: effect of fluid flow on the microstructure of LM24 die-casting alloy. J Mater Process Technol. 1995;52(2-4):193-206.

6. Ghomashchi MR, Vikhrov A. Squeeze casting: an overview. J Mater Process Technol. 2000;101(1-3):1-9.

7. Führ LT, Ludwig GA, Martins MR, Vecchia FD, Rieder E, Malfatti C, et al. Effects of mold temperature in squeeze casting of Zamak 5. Mater Sci Forum. 2014;775-776:729-32.

8. Oliveira CT. Caracterização microestrutural e eletroquimica de óxidos de nióbio crescidos por anodização [tese]. Programa de Pós-graduação em Engenharia de Minas, Metalúrgica e de Materiais, Escola de Engenharia, Universidade Federal do Rio Grande do Sul, Porto Alegre; 2007.

9. Lilov E, Lilova V, Girginov C, Kozhukharov S, Tsanev A, Yancheva D. Induction periods during anodic polarization of zinc in aqueous oxalic acid solutions. Mater Chem Phys. 2019;223:727-36.

10. El-Mahdy GA. Formation and dissolution behavior of niobium oxide in phosphoric acid solutions. Thin Solid Films. 1997;307(1-2):141-7.

11. Khera S, Chand P. Influence of different solvents on the structural, Optical, Impedance and Dielectric Properties of ZnO Nanoflakes. Zhongguo Wuli Xuekan. 2019;57:28-46.

12. Handore K, Bhavsar S, Horne A, Chhattise P, Mohite K, Ambekar J, et al. Novel green route of synthesis of ZnO nanoparticles by using natural biodegradable polymer and its application as a catalyst for oxidation of aldehydes. Journal of Macromolecular Science Part A. 2014;51(12):941-7.

13. Shamsipur M, Roushani M, Pourmortazavi SM. Electrochemical synthesis and characterization of zinc oxalate nanoparticles. Mater Res Bull. 2013;48(3):1275-80.

14. Zhang XG. Passivation and surface film formation. In: Zhang XG. Corrosion and electrochemistry of zinc. Boston: Springer; 1996.

15. Zhang XG. Properties, products and processes. In: Zhang XG. Corrosion and electrochemistry of zinc. Boston: Springer; 1996.

16. Reveko V, Moller P. Special aspects of electrodeposition on zinc die castings. Nasf Surface Technology White. 2018;82(8):1-9.

17. Ferreira JMJ Jr, Oliveira M, Trindade GF, Santos LCL, Tomachuk CR, Baker MA. Development and characterization of zinc oxalate conversion coatings on zinc. Corros Sci. 2018;137:13-32.

18. Choudhary RK, Mishra P, Kain V, Singh K, Kumar S, Chakravartty JK. Scratch behavior of aluminum anodized in oxalic acid: effect of anodizing potential. Surf Coat Tech. 2015;283:135-47.

19. Kao T-T, Chang Y-C. Influence of anodization parameters on the volume expansion of anodic aluminum oxide formed in mixed solution of phosphoric and oxalic acids. Appl Surf Sci. 2014;288:654-9.

20. Roslyakov IV, Kolesnik IV, Levin EE, Katorova NS, Pestrikov PP, Kardash TY, et al. Annealing induced structural and phase transitions in anodic aluminum oxide prepared in oxalic acid electrolyte. Surf Coat Tech. 2020;381:125159.

21. Mehdizade M, Soltanieh M, Eivani AR. Investigation of anodizing time and pulse voltage modes on the corrosion behavior of nanostructured anodic layer in commercial pure aluminum. Surf Coat Tech. 2019;358:741-52.

22. Xing J, Lu S, Zhang C, Yin M, Li D, Song Y. Determination of the field strength and realization of the high-field anodization of aluminum. Phys Chem Chem Phys. 2017;19(32):21696-706.

23. Kato T, Nunome K, Kaneko K, Saka H. Formation of the ζ-phase at a 468 interface between a Fe substrate and a molten 0.2 mass% Al–Zn during 469 galvannealing. Acta Mater. 2000;48(9):2257-62.

24. Goodwin F, Rollez D. Zinc alloys. In: Wiley-VCH. Ullmann's encyclopedia of industrial chemistry. Hoboken: Wiley-VCH Verlag GmbH & Co; 2014. p. 1-7. http://dx.doi.org/10.1002/14356007. a28_531.pub2.

25. Zhang R, Jiang K, Zhu Y, Qi H, Ding G. Ultrasound-assisted anodization of aluminum in oxalic acid. Appl Surf Sci. 2011;258(1):586-9.

26. Feliu S Jr, Barranco V. XPS study of the surface chemistry of 474 conventional hot-dip galvanized pure Zn, galvanneal and Zn–Al alloy 475 coatings on steel. Acta Mater. 2003;51(18):5413-24.

27. Cao Z, Kong G, Che C, Wang Y. Influence of Nd addition on the corrosion behavior of Zn-5%Al alloy in 3,5wt.% NaCl solution. Surf Sci. 2017;426:67-76.

28. Mehrabian M, Nayebi B, Dietrich D, Lampke T, Shokouhimehr M. Characteristics of dynamically-formed surface oxide layers on molten zinc–aluminum alloys: a multimodality approach. Thin Solid Films. 2018;667:34-9.

29. Gilani S, Ghorbanpour M, Parchehbaf Jadid A. Antibacterial activity of ZnO films prepared by anodizing. Journal of Nanostructure in Chemistry. 2016;6(2):183-9.

30. Gancarz T, Mech K, Guśpiel J, Berent K. Corrosion studies of Li, Na and Si doped Zn-Al alloy immersed in NaCl solutions. J Alloys Compd. 2018;767:1225-37.

31. Mouanga M, Berçot P, Rauch JY. Comparison of corrosion behaviour of zinc in NaCl and in NaOH solutions. Part I: corrosion layer characterization. Corros Sci. 2010;52(12):3984-92.

32. Abd El Aal EE. Limits determination of toleration of aggressive anions by a certain passivator on zinc surface. Corros Sci. 2008;50(1):47-54.

33. Liu J-C, Park SW, Nagao S, Nogi M, Koga H, Ma J-S, et al. The role of Zn precipitates and Cl⁻ anions in pitting corrosion of Sn-Zn solder alloys. Corros Sci. 2015;92:263-71.